Kinetics and mechanism of adsorption of methylene blue from aqueous solution by nitric-acid treated water-hyacinth

Mohammad I. El-Khaiary *

Chemical Engineering Department, Faculty of Engineering, Alexandria University, El-Hadara, Alexandria 21544, Egypt

Abstract

Kinetics adsorption experiments were conducted to evaluate the adsorption characteristics of a cationic dye (methylene blue, MB) onto nitric-acid treated water-hyacinth (N-WH). Results showed that N-WH can remove MB effectively from aqueous solution. The loading of MB onto N-WH was found to increase significantly with increasing the initial MB concentration, but the residual concentration of MB in solution also increased. A complete removal of MB from solution was only achieved at the lower range of initial MB concentration (less than 286 mg/L). Temperature had a slight effect on the amount adsorbed at equilibrium. The adsorption rate was fast and more than half of the adsorbed-MB was removed in the first 15 min at room temperature, which makes the process practical for industrial application. The adsorption kinetics at room temperature could be expressed by the pseudo second order model, while at higher temperatures (45–80 °C) and low MB concentration (97 mg/L) both Lagergren's model and the pseudo second order model can be used to predict the kinetics of adsorption. The overall rate of dye uptake was found to be controlled by external mass transfer at the beginning of adsorption, then gradually changed to intraparticle diffusion control at a later stage. The initial period where external mass transfer is the rate controlling step was found to increase with increasing initial MB concentration and decrease with increasing temperature. The increase in temperature was also found to increase the rate of adsorption and reduce the time required to reach equilibrium. The initial rate of adsorption, h_o, was calculated, it was found to increase with increasing temperature, while the increase in MB concentration decreased h_o at the lower concentration range then increased h_o again at high concentration. The value of the activation coefficient, E, was found to be 8.207 kJ/mol, which indicates a diffusion controlled process.
© 2007 Published by Elsevier B.V.

Keywords: Adsorption; Dye; Methylene blue; Water-hyacinth; Biosorption; Kinetics

1. Introduction

In industrial water pollution, the color produced by small concentrations of synthetic dyes in water is important, because besides having possible toxic effects, the color in water is visibly unpleasant. The effluents from textile dyeing and similar industries are generally highly colored, with large amounts of suspended organic solids. Synthetic dyes are designed to be stable to biodegradation and therefore biological treatment processes are ineffective in removing color from wastewater, moreover, degradation products of some dyes are toxic. Adsorption is widely used to remove pollutants from waste water. Activated carbon has been used widely as an adsorbent for the removal of many pollutants, but activated carbon is expensive

and not easily regenerated [1]. Therefore, low-cost adsorbents that are able to adsorb pollutants have been extensively tested [2–4]. The use of agricultural solid wastes not only transforms the waste into useful material, but also mitigates the problem of disposal of these wastes. Many plant biosorbents were tested for their ability to adsorb MB from aqueous solutions [5–11], a comparison of their MB adsorption capacities is given in Table 1.

Water-hyacinth (WH) (Eichornia Crassipes) is a wild fern belonging to the Family Pontederiaceae. A native to South America, it has been naturalized in many tropical and subtropical regions of the world. It first appeared in Egypt in the 1890s [12], then it has invaded many water ways including African rivers and Lake Victoria [13]. WH grows and reproduces in a very high rate and is considered the worst aquatic plant [14]. The dense mats of WH float on the water surface, blocking navigation and interfere with irrigation, fishing, recreation, and power generation. These mats also prevent sunlight penetration and reduce the aeration of water, leading to oxygen deficiency, competitively

* Tel.: +20 12175916; fax: +20 34240043.
  E-mail address: El-Khaiary@rocketmail.com.

Table 1
Comparison of methylene blue adsorption capacity by different plant biosorbents, q_m values determined from the Langmuir isotherm

q_m (mg/g)	Adsorbent	References
915	Bark	[4]
312	Rice husk	[4]
278	Cotton waste	[4]
153	Mango sees kernel	[5]
128.9	Water-hyacinth root	[6]
119	Giant duckweed	[7]
99	Coconut husk	[8]
80.3	Date pits	[9]
32.3	Modified sawdust	[10]
20.8	Banana peel	[11]
18.06	Orange peel	[11]

exclude submerged plants, and reduce biological diversity. A large amount of funding (especially from the World Bank) has so far not been able to stop the wide spread WH invasion. At the present time, the Egyptian government is trying to control the WH invasion, mainly by mechanical collection and dumping. This method is expensive and presents a solid waste problem to get rid of the WH dumps. Much research has been conducted in efforts to create a use for dumped WH. This includes research on biogas generation [15], fish feed [14], and animal feed [16]. These attempts have not yet been successful in utilizing WH on an industrial scale.

In this study the waste WH, after treatment with nitric-acid, was used and evaluated as a possible biosorbent for the removal of a cationic dye (methylene blue, MB) from aqueous solution. The objective of this study is to investigate the effect of initial MB concentration, temperature, and contact time on the adsorption process. Kinetics and mass transfer studies have been performed and the results have been analyzed by applying conventional theoretical methods.

2. Materials and methods

2.1. Adsorbent preparation

Live WH was collected from El-Mahmoudeya Canal, Alexandria, Egypt. Live WH consists of 94–95% water and barely contains 50–60 g total solid per kilogram [15]. The plants were thoroughly washed with water, the roots were cut out and disposed, then the leaves and stems were left to dry in the sun for 14 days. In a recent publication, the sun-dried WH of El-Mahmoudeya Canal near Alexandria was analyzed [14]. It was found to contain 19% crude fiber, 18.2% ash, 21.1% crude protein, 1.0% crude lipids, and 40.7% nitrogen-free extract. In the present study, the sun-dried WH was subjected to washing and chemical treatment with nitric-acid to remove soluble compounds and to alter the surface properties.

The sun-dried WH was soaked in 2 M AR grade nitric-acid for 24 h. The ratio of nitric-acid solution to WH was 10 mL/g. It was then washed repeatedly with hot distilled water until the filtrate was free of nitrate. It was subsequently dried at 105 °C for 24 h, then ground and sieved to particle size 0.20–0.315 mm, and stored in a desiccator.

2.2. Methylene blue

Methylene blue ($C_{16}H_{18}N_3Cl \cdot 3H_2O$) was purchased from Sigma–Aldrich and used without further purification. All MB solutions used in this study were prepared by weighing and dissolving the required amounts MB in distilled water.

2.3. Adsorption kinetic experiments

Kinetic adsorption experiments were carried out to investigate the effect of time on the adsorption process and to identify the adsorption rate. The experimental procedure was as follows: (1) several 1.5 L of MB solutions of various concentrations (97–1187 mg/L) were prepared. (2) The MB solution was placed into a thermostatically controlled 2 L beaker equipped with 4 vertical baffles, each baffle 1 cm wide and going the full length of the beaker. The temperature was controlled to ±2 °C. (3) Three grams of nitric-acid treated water-hyacinth (N-WH) were added to the solution and stirred by a rectangular impeller (0.5 cm × 5 cm) at 800 rpm. (4) Five milliliter samples were withdrawn at time intervals, the solid was separated by decantation, and the residual MB concentration in solution was measured immediately using Novaspec LKB spectrophotometer (Pharmacia) at wave length 655 nm. The amount of dye adsorbed was determined from the difference in concentration between samples withdrawn. The stirring was continued until the concentration of MB blue was constant.

3. Results and discussion

3.1. Effect of initial methylene blue concentration

Fig. 1 shows the effect of initial MB concentration, C_o, on the kinetics of adsorption of the dye at natural pH (3.7–4.4), N-WH dosage 2 g/L, and 27 °C. An increase in the initial MB concentration leads to a decrease in the MB removal. As the initial MB concentration increases from 97.2 to 1187.2 mg/L the equilibrium removal of MB decreases from 99 to 54%. It is also noticed in Fig. 1 that large fractions of the total amount
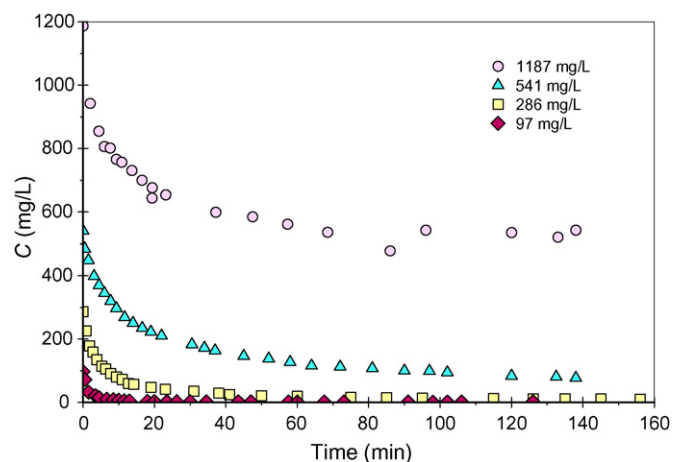

Fig. 1. The adsorption kinetics of MB on N-WH for different initial concentrations at 27 °C, natural pH (3.7–4.4) and N-WH dose: 2 g/L.

adsorbed of MB were removed in the initial rapid uptake phase. In the first 10 min, the fractions of total amounts adsorbed are about 93, 73, 47, and 36% for initial MB concentrations 97, 286, 541, and 1187, respectively. This is due to the high concentration gradient in the beginning of adsorption which represents a high driving force for the transfer of MB from solution to the surface of N-WH.

The transient behavior of the system at different initial MB concentrations was analyzed using the Lagergren's pseudo first order [17] and Ho's pseudo second order models [18]. The Lagergren equation, a pseudo-first-order equation, describes the kinetics of adsorption process as follows:

$$\frac{dq}{dt} = k_1(q_e - q) \tag{1}$$

where q_e is the amount of adsorbate adsorbed at equilibrium (mg/g), q the amount of adsorbate adsorbed at time t (mg/g) and k_1 is the rate constant of pseudo-first order adsorption (min^{-1}). Since $q = 0$ at $t = 0$, the initial rate of adsorption can be calculated from Eq. (1) as follows:

$$h_{o,1} = k_1 q_e \tag{2}$$

By integrating Eq. (1) for the boundary conditions $t = 0$ to $t = t$ and $q = 0$ to $q = q$, gives:

$$q = q_e(1 - e^{-k_1 t}) \tag{3}$$

On the other hand, the pseudo second order kinetic equation of Ho based on adsorption capacity may be expressed in the form:

$$\frac{dq}{dt} = k_2(q_e - q)^2 \tag{4}$$

where k_2 is the rate constant of pseudo second order adsorption (g/mg min) and q_e is the amount of solute adsorbed at equilibrium (mg/g). Integrating Eq. (3) for boundary conditions $t = 0$ to $t = t$ and $q = 0$ to $q = q$ gives:

$$q = \frac{q_e^2 k_2 t}{1 + q_e k_2 t} \tag{5}$$

and the initial rate of adsorption $h_{o,2}$ is:

$$h_{o,2} = k_2 q_e^2 \tag{6}$$

The experimental results of the dye uptake, q, versus time were fitted to both models by the method of nonlinear regression. The regression results are shown in Table 2 and Figs. 2 and 3. It can be seen from the plots of q versus t that an increase in initial MB concentration leads to an increase in the adsorption
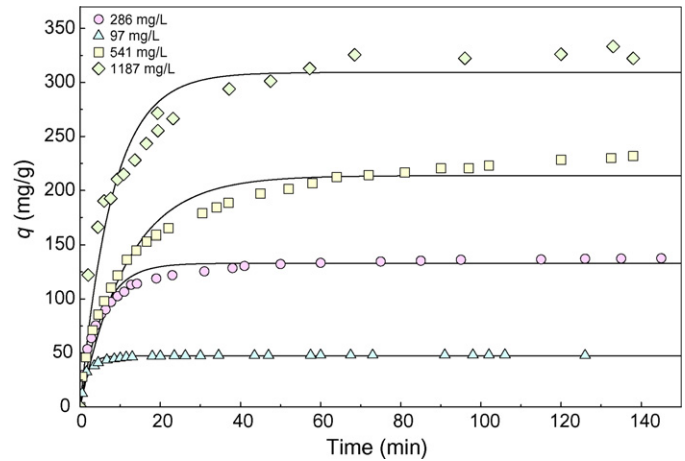

Fig. 2. The fitting of Lagergren's model for MB adsorption on N-WH at different initial concentrations at 27 °C, natural pH (3.7–4.4) and N-WH dose: 2 g/L.
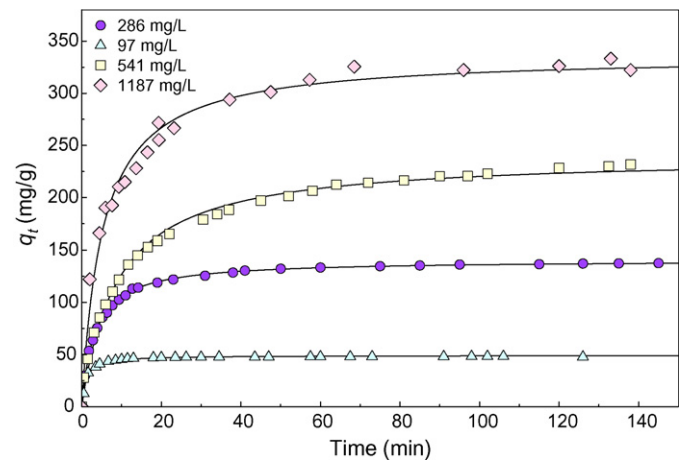

Fig. 3. The fitting of pseudo second order model for MB adsorption on N-WH at different initial concentrations at 27 °C, natural pH (3.7–4.4) and N-WH dose: 2 g/L.

capacity, q_e. As the initial MB concentration increases from 97 to 1187 mg/L, the experimentally observed adsorption capacity, q_{exp}, increases from 48.2 to 333 mg/g. This indicates that the initial dye concentration plays an important role in determining the adsorption capacity of MB on N-WH. This may be related to the solution state of MB at different concentrations. In the beginning of the adsorption process, the MB is adsorbed on the external surface of N-WH particle, which increases the local concentration of MB on the surface and leads to the formation of MB aggregates. MB molecules are known to form dimmers and aggregates, depending on the conditions of solution such

Table 2
Pseudo first order and pseudo second order rate constants at 27 °C and different initial MB concentrations (C_o: mg/L; q_e: mg/g; h_o: mg/g min; k_1: min^{-1}; k_2: g/mg min)

C_o	q_{exp}	Lagergren's pseudo first order model				Pseudo second order model			
		q_e	k_1	$h_{o,1}$	R^2	q_e	k_2	$h_{o,2}$	R^2
97	48.27	47.110	0.5859	27.65	0.9827	49.159	0.02072	50.06	0.9922
286	138.6	133.00	0.1868	24.84	0.9647	140.54	0.002151	42.47	0.9990
541	231.8	213.72	0.08402	17.96	0.9626	240.05	0.0004653	26.51	0.9934
1187	333.2	309.18	0.1245	38.49	0.9287	336.50	0.0005698	64.52	0.9835

as pH, concentration, temperature, and presence of other ions [19,20]. MB aggregates can migrate from the external surface of N-WH to the internal pores, resulting in deaggregation of the MB aggregates and restoring monomers. At high loading rates of MB, it is expected that agglomerates are predominant in solution, while monomers and dimers are virtually absent in the MB-adsorbent complexes on the solid surface.

It is observed from Fig. 2 that for all initial MB concentrations, the adsorption data were well represented by Lagergren's model of Eq. (3) only for the initial period of adsorption (5–15 min), and thereafter it deviates from theory. The values of adsorption capacity, q_e, calculated from Lagergren's model are lower than the values observed experimentally, q_{exp}, with the difference increasing with the increase of initial MB concentration. By examining the values of the coefficient of determination, R^2, it is noticed that the fitting at 97 mg/L has the highest R^2 value of 0.9827, with values of R^2 decreasing at higher initial MB concentration to reach a value of 0.9287 when C_o is 1187 mg/L. This means that it is not appropriate to use Lagergren's model for the prediction of the kinetics of MB adsorption on N-WH for the entire time period of adsorption and all initial MB concentrations.

The kinetic data were further analyzed using the pseudo second order model of Eq. (5). By comparing Figs. 2 and 3, it is obvious that the pseudo second order model fits the experimental data better than Lagergren's model for the entire adsorption period. Also, from the regression results in Table 2, the values of q_e obtained from the pseudo second order model are closer to the experimental results than q_e obtained from Lagergren's model. By comparing the coefficient of determination, R^2, in Table 2, it is observed that the pseudo second order model fits the experimental results with higher R^2 values (0.9835–0.9990) than Lagergren's model (R^2 from 0.9287–0.9827). The higher R^2 values confirm that the adsorption kinetics data are well represented by the pseudo second order model, thus supporting the basic assumption in the model that chemisorption plays a major role in this adsorption system.

It is also observed in Table 2 that when the MB initial concentration increases from 97 to 541 mg/L, the rate constant, k_2, decreases from 0.0207 to 0.00046 mg/g min, but further increase in initial concentration to 1187 mg/L causes k_2 to reverse the trend and increase to 0.00056. This may be related to the aggregation state of MB as discussed above. The values of the initial sorption rate, $h_{o,2}$, are also shown in Table 2. When the initial MB concentration increases from 97 to 541 mg/L, values of $h_{o,2}$ decrease from 50.0 to 26.5 mg/g min, but a further increase of initial concentration to 1187 mg/L causes $h_{o,2}$ to reverse the trend and increase to 64.5 mg/g min.

Further, in order to differentiate the kinetic rate constants obtained from the Lagergren pseudo first order and from the pseudo second order kinetic models, the values of k_1 and k_2 are plotted against the initial MB concentration in Fig. 4. It is observed from the figure that there is no linear relationship between the rate constants and the initial MB concentration, but the trend patterns are exactly the same for k_1 and k_2. The nonlinear relationships between initial MB concentration and the rate constants suggest that several mechanisms play roles
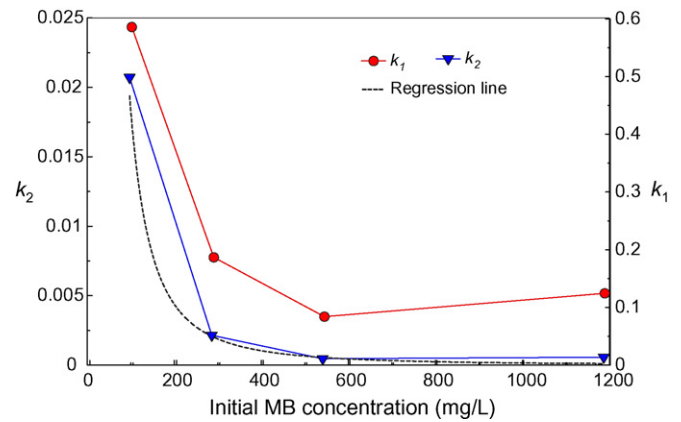

Fig. 4. Plot between the kinetic constants of Lagergren's and pseudo second order models against C_o.

in the adsorption process, such as ion exchange, chelation, and physical adsorption. As it was determined that the pseudo second order model is better in predicting the adsorption kinetics at 27 °C and different values of C_o, the values of $q_{e,2}$, k_2, and $h_{o,2}$ were correlated with the initial MB concentration to obtain expressions for these values in terms of C_o as follows:

$$q_e = 0.6130 + 0.5927C_o - 0.00256C_o^2, \quad R^2 = 0.9999 \quad (7)$$

$$k_2 = \frac{1}{1 + 0.07092C_o^2}, \quad R^2 = 0.9990 \quad (8)$$

$$h_{o,2} = 62.39 - 0.1137C_o + 9.7 \times 10^{-5}C_o^2, \quad R^2 = 0.9542 \quad (9)$$

Substituting the above equations into Eq. (5), the relationship of q, C_o, and t can be expressed as follows:

$$\frac{1}{q} = \frac{1}{(62.39 - 0.1137C_o + 9.7 \times 10^{-5}C_o^2)t} + \frac{1}{0.613 + 0.5927C_o - 0.00256C_o^2} \quad (10)$$

Eq. (10) can be used to predict the amount of MB adsorbed on N-WH for any given C_o and contact time, at natural pH (3.7–4.4), and N-WH dose 2 g/L.

3.2. Sorption mechanism

Although the kinetic studies help in identifying the adsorption process, the determination of the sorption mechanism is important for design purposes. Considering a solid–liquid adsorption process, the adsorbate transfer is characterized by either boundary layer diffusion (external mass transfer) or intraparticle diffusion (mass transfer through the pores), or by both. It is generally accepted that the adsorption dynamics consists of three consecutive steps:

• Transport of adsorbate molecules from the bulk solution to the adsorbent external surface through the boundary layer diffusion.

- Diffusion of the adsorbate from the external surface into the pores of the adsorbent.
- Adsorption of the adsorbate on the active sites on the internal surface of the pores.

The last step, adsorption, is usually very rapid in comparison to the first two steps. Therefore, the overall rate of adsorption is controlled by the first or second step, whichever is slower, or a combination of both. Many studies have shown that the boundary layer diffusion is the rate controlling step in systems characterized by dilute concentrations of adsorbate, poor mixing, and small particle size of adsorbent. Whereas the intraparticle diffusion controls the rate of adsorption in systems characterized by high concentrations of adsorbate, vigorous mixing, and large particle size of adsorbent [21]. Also, it has been noticed in many systems that boundary layer diffusion (external mass transfer) is dominant at the beginning of adsorption during the initial adsorbate uptake, then gradually the adsorption rate becomes controlled by intraparticle diffusion as the adsorbent's external surface becomes loaded with the adsorbate.

The intraparticle diffusion parameter, k_i (mg/g min$^{0.5}$) is defined by the following equation [22]:

$$q = k_i t^{0.5} + c \tag{11}$$

where q is the amount of MB adsorbed (mg/g) at time t, k_i the intraparticle diffusion constant (mg/g min$^{0.5}$), and c is the intercept.

Theoretically, the plot of k_i versus $t^{0.5}$ should show at least four linear regions that represent boundary layer diffusion, followed by intraparticle diffusion in macro, meso, and micro pores [23]. These four regions are followed by a horizontal line representing the system at equilibrium. The intraparticle diffusion plots of the experimental results, q versus $t^{0.5}$ for different initial MB concentrations at 27 °C and N-WH dose of 2 g/L are shown in Fig. 5. From the figure it is observed that there are three linear regions and one curved region. At the beginning of adsorption there is a linear region representing the rapid sur-
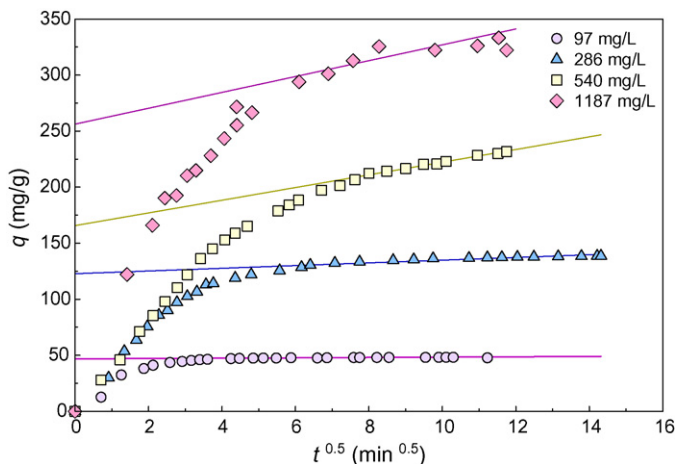

Fig. 5. Intraparticle diffusion plot for the adsorption at 27 °C and different initial MB concentrations (pH 3.7–4.4; N-WH dose: 2 g/L).

Table 3
Diffusion coefficients for adsorption of MB on N-WH at 27 °C, natural pH (3.3–3.5) and different initial concentrations (C_o: mg/L; c: mg/g; k_i: mg/g min$^{0.5}$; k_s: min^{-1}; D_i: m^2/s)

C_o	c	k_i	k_s	D_i
97	46.83	0.1488	0.4734	3.014×10^{-8}
286	122.8	1.206	0.2188	1.420×10^{-8}
541	165.7	5.657	0.1439	8.731×10^{-9}
1187	261.6	6.280	0.1106	8.389×10^{-9}

face loading, followed by a curved portion where the overall rate is controlled by both film-diffusion and pore diffusion, then a linear region representing pore diffusion, and finally a horizontal linear region representing equilibrium. It is observed that the time elapsed until pore diffusion starts controlling the rate of adsorption increases from 26 to 58 min when the initial MB concentration increases from 97 to 541 mg/L, on further increase of initial MB concentration to 1187 mg/L the elapsed time to the start of diffusion control drops to 37 min. This is similar to the trend of the initial adsorption rate, $h_{o,1}$ and, $h_{o,2}$ shown in Table 2. The intraparticle diffusion parameter, k_i, is determined from the slope of the second linear region while the intercept is proportional to the boundary layer thickness. The calculated values of k_i and the intercept are shown in Table 3. It is obvious that values of k_i increase from 0.1488 to 6.280 when the initial MB concentration is increased from 97 to 1187 mg/L. It is also observed that the value of the intercept increases from 46.83 to 261.6 when C_o is increased from 97 to 1187 mg/L, which indicates that the thickness of the boundary layer increases significantly with increase of C_o.

The multilinear nature of the intraparticle diffusion plots suggests the predominance of external mass transfer of MB at the beginning of adsorption [24]. The rate constants of external mass transfer were calculated using the plot of C/C_o against time at different initial MB concentrations (figure not shown). The experimental results were fitted to a second order polynomial, then the slopes were calculated from the first derivative of the polynomial functions. The values of initial adsorption rates, k_s (min^{-1}) are shown in Table 3. It is observed that the rate in the initial period of adsorption, where external mass transfer is assumed to predominate, decreases with increase of C_o, which can be expected due to the increase in boundary-layer thickness exhibited in the values of the intercept in intraparticle diffusion plots. The decrease of k_s with increasing C_o is not in agreement with the trends of h_o for Lagergren's and pseudo second order models. The reason for this discrepancy may be because the fitting of the pseudo kinetics models was performed on the experimental results of the entire time period of adsorption, thus the estimates for the initial stage was affected by the experimental results of later stages occurring after a relatively long time. The relationship between k_s and C_o fits the equation:

$$k_s = \frac{1}{1 + 0.0121 C_o^{0.9928}}, \quad R^2 = 0.9794 \tag{12}$$

In order to determine the actual rate controlling steps in MB adsorption on N-WH, the experimental data was further
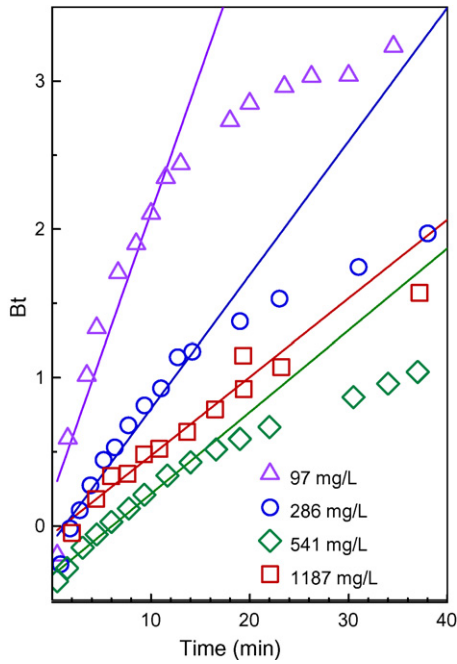
Fig. 6. Boyd plots for MB adsorption at 27 °C and different initial MB concentrations (pH 3.7–4.4; N-WH dose: 2 g/L).

analyzed by the expression of Boyd et al. [25]:

$$F = 1 - \frac{6}{\pi^2} \exp(-Bt) \tag{13}$$

where F is the fractional attainment of equilibrium, at different times, t, and Bt is a function of F.

$$F = \frac{q_t}{q_e} \tag{14}$$

where q_t and q_e are the dye uptake (mg/g) at time t and at equilibrium, respectively.

Eq. (13) can be rearranged to

$$Bt = -0.4977 - \ln(1 - F) \tag{15}$$

The values of Bt were calculated from Eq. (15) and plotted against time as shown in Fig. 6. The plots are linear only in the initial period of adsorption and does not pass through the origin, indicating that external mass transfer is the rate limiting process in the beginning of adsorption. The calculated values of B were used to determine the effective diffusion coefficient, D_i, (cm^2/s)
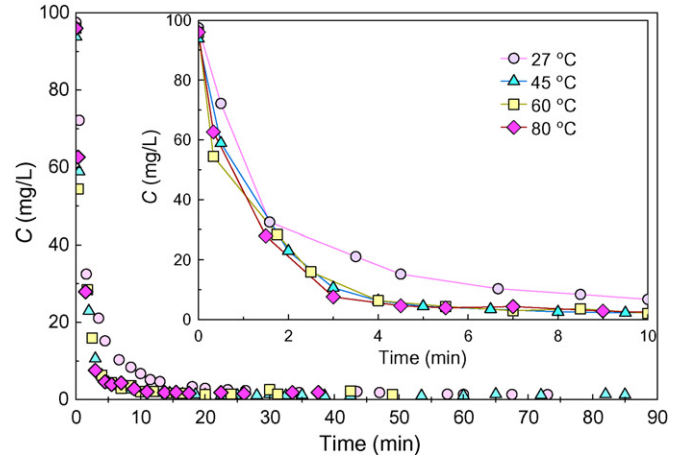

Fig. 7. Effect of temperature on the adsorption of MB on N-WH for different initial concentrations (pH 3.7–4.4; N-WH dose: 2 g/L; C_o: 97 mg/L).

from the equation:

$$B = \frac{\pi^2 D_i}{r^2} \tag{16}$$

where r is the radius of the N-WH particle assuming spherical shape. The values of D_i in Table 3 show that the effective diffusion coefficient decreases with increasing initial MB concentration. Also, by examining Fig. 6, it is obvious that the initial period where external mass transfer is the rate controlling step increases from 13 to 23 min when C_o increases from 97 to 1187 mg/L.

3.3. Effect of temperature

Fig. 7 shows the effect of temperature on the adsorption of MB on N-WH at natural pH (3.7–4.4), N-WH dosage 2 g/L, initial MB concentration 97 mg/L, and different temperatures. It can be seen from the figure that the time needed to reach equilibrium decreases at higher temperatures, so that at 27, 45, 60, and 80 °C the times needed to reach equilibrium are about 100, 25, 20, and 15 min, respectively. It can also be seen in Fig. 7 that the increase in temperature leads to slight changes in MB removal, so at temperatures 27, 45, 60, and 80 °C the percent removal of MB values are 99, 98.6, 98.1, and 98.2, respectively.

Table 4 and Figs. 8 and 9 show the nonlinear regression results of fitting the observed values of q against t according to Lagergren's model and the pseudo second order model. By examining

Table 4
Pseudo first order and pseudo second order rate constants, initial MB concentration: 97 mg/L, and different temperatures (C_o: mg/L; q_e: mg/g; h_o: mg/g min; k_1: min^{-1}; k_2: g/mg min)

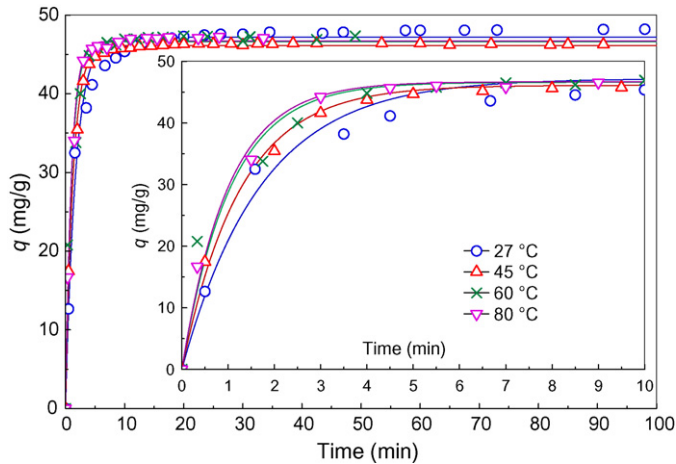| T (°C)	q_{exp}	Lagergren's pseudo first order model					Pseudo second order model			
		q_e	k_1	$h_{o,1}$	R^2		q_e	k_2	$h_{o,2}$	R^2
27	48.27	47.19	0.5859	27.65	0.9827		49.16	0.02072	50.06	0.9922
45	46.25	46.11	0.7970	36.75	0.9983		47.66	0.03371	76.57	0.9837
60	47.10	46.06	0.9571	44.60	0.9649		48.46	0.04140	97.23	0.9892
80	47.15	46.69	1.001	47.46	0.9928		49.54	0.03517	86.32	0.9910

Fig. 8. The fitting of Lagergren's model for MB adsorption on N-WH at different temperatures (pH 3.7–4.4; N-WH dose: 2 g/L; C_o: 97 mg/L).

the values of R^2 for the fitting to Lagergren's model, it can be seen that the R^2 values are high (0.9827–0.9983), unless at 60 °C where R^2 is 0.9649. These values are almost like R^2 for the fitting to the pseudo second order model (0.9837–0.9922). However, by comparing the predicted values of q_e with the experimental results, it is clear that Lagergren's model slightly underestimates q_e, while the q_e predictions from the pseudo second order model are significantly higher than the experimental results. This comparison indicates that at the higher temperature range and low MB concentration, both models can be used to predict the kinetics of adsorption of MB on N-WH, the Lagergren's model being slightly better in estimating the equilibrium MB uptake. The small changes in q_{exp} with change in temperature can be observed in Table 4. The equilibrium dye uptake decreases from 48.27 to 46.25 mg/g when the temperature is raised from 27 to 45 °C, suggesting an exothermic adsorption in the temperature range 27–45 °C. However, when the temperature is increased from 45 to 80 °C the value of q_{exp} increases from 46.25 to 47.15 mg/g, suggesting a slightly endothermic adsorption in the temperature range from 45 to 80 °C. This change in the heat of
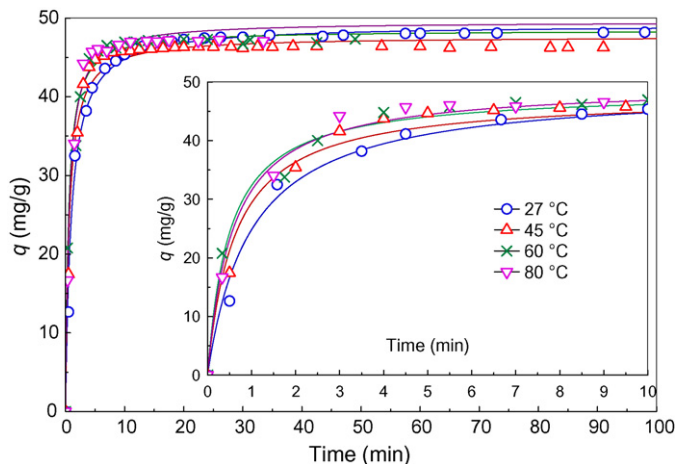
adsorption may be due to several reasons, on the solution side the aggregation state of MB is temperature dependant, and on the N-WH side the ionization of the various surface groups are also expected to change with the change in temperature.

The pseudo first order rate constant is expressed as a function of temperature by an Arrhenius type relationship as follows:

$$k_1 = k_o \exp\left(\frac{-E}{RT}\right) \tag{17}$$

where k_o is a temperature independent factor (g/mg min), E the activation energy of adsorption (J/mol), R the universal gas constant (8.314 J/mol K) and T is the absolute temperature (K). The activation energy was calculated according to Eq. (17) and was found to be 8.446 kJ/mol. The low values of activation energy (5–40 kJ/mol) are characteristic for physisorption, while higher values (40–800 kJ/mol) suggest chemisorption [26]. Therefore, the value of E obtained in the present study shows that the adsorption of MB on N-WH is mainly a physical process.

The values of the initial sorption rates calculated from the Lagergren's model, $h_{o,1}$, and from the pseudo second order model, $h_{o,2}$, are shown in Table 4. It is noticed from the table that $h_{o,1}$ increases constantly with increasing temperature, having values of 0.5859, 0.7970, 0.9571, and 1.001 at temperatures 27, 45, 60, and 80 °C, respectively. On the other hand, $h_{o,2}$ shows a different trend, the values initially increase with temperature so that at 27, 45, and 60 °C, values of $h_{o,2}$ are 0.02072, 0.03371, and 0.04140, respectively, but with further increase of temperature to 80 °C, $h_{o,2}$ decreases to 0.03517. The discrepancy between the trends of $h_{o,1}$ and $h_{o,2}$ can be resolved by calculating the initial rate of adsorption by other methods, as shown in Section 3.4.

3.4. Effect of temperature on sorption mechanism

Fig. 10 shows the intraparticle diffusion plots for the adsorption of MB on N-WH at different temperatures, C_o 97 mg/L,

Fig. 9. The fitting of the pseudo second order model for MB adsorption on N-WH at different temperatures (pH 3.7–4.4; N-WH dose: 2 g/L; C_o: 97 mg/L).
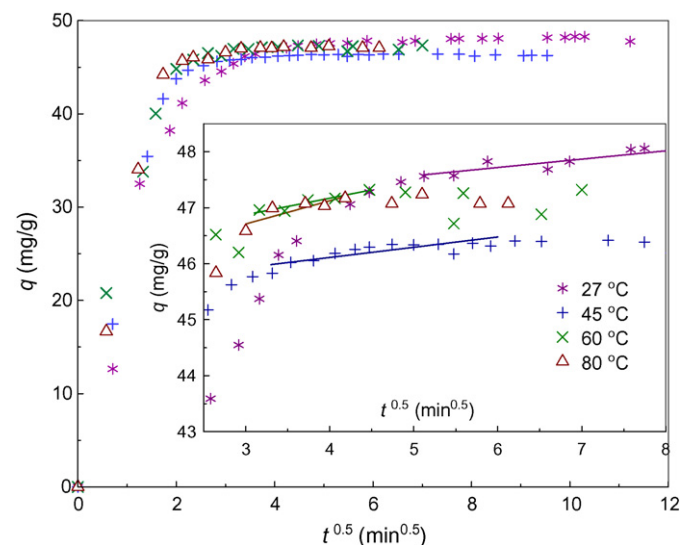

Fig. 10. Intraparticle diffusion plot for the adsorption of MB at different temperatures (pH 3.7–4.4; N-WH dose: 2 g/L; C_o: 97 mg/L).

Table 5
Diffusion coefficient for adsorption of MB on N-WH at different temperatures, natural pH (3.3–3.5) and initial MB concentration 97 mg/L (T: °C; k_i: mg/g min$^{0.5}$; k_s: min^{-1}; D_i: m^2/s)

T	c	k_i	k_s	D_i
27	46.83	0.1488	0.4734	3.014×10^{-8}
45	45.38	0.1827	0.4952	6.765×10^{-8}
60	45.99	0.2961	0.5492	7.558×10^{-8}
80	45.46	0.4150	0.7087	9.191×10^{-8}

N-WH dosage 2 g/L, and natural pH (3.7–4.4). The same multilinear plots that were observed when C_o was varied at 27 °C are also observed in Fig. 10 at different temperatures and constant C_o. It is observed from the figure that the start of the second linear region, where the rate is assumed to be controlled by intraparticle diffusion, is dependent on temperature. The intraparticle diffusion controlled region at 27 °C started after 26 min, while the time decreased with increasing temperature to be 11, 10, and 9 min at 45, 60, and 80 °C, respectively. This would be expected due to the decreased viscosity of aqueous MB solution, and also the effect of heating on increasing the diffusion of molecules in solution. Both factors enhance the diffusion of MB through the boundary layer, therefore, the initial film-diffusion controlled time period becomes shorter at higher temperatures. It can also be seen from Table 5 that the values of the intraparticle diffusion constant increase with increasing temperature. The values of k_i are 0.1488, 0.1827, 0.2961, and 0.4150 mg/g min$^{0.5}$ at temperatures 27, 45, 60, and 80 °C, respectively. This is probably due to the swelling of fibers at higher temperatures, which facilitates dye diffusion inside the adsorbent particle.

The rate constants of external mass transfer were calculated using the plots of C/C_o against time at different initial MB concentrations (figure not shown). The experimental results were fitted to second order polynomial, then the slopes were calculated from the first derivative of the polynomial functions. The values of initial adsorption rates, k_s (min^{-1}), are shown in Table 5. It is observed that the adsorption rate in the initial period, where external mass transfer is assumed to predominate, increases with increasing temperature. The relationship between k_s and T (°C) fits the equation:

$$k_s = 0.5727 - 0.006335T + 1.003 \times 10^{-4}T^2, \quad R^2 = 0.9987 \tag{18}$$

The plots of Bt against time at different temperatures are shown in Fig. 11 and the values of D_i are presented in Table 5. It is observed from the figure that the plots are linear in the initial period of adsorption, with the time duration of the linear period decreasing with increase of temperature. The initial adsorption period, assumed to be controlled by external mass transfer lasted for 13, 6.5, 5.5, and 4.5 min at temperatures 27, 45, 60, and 80 °C, respectively. It is also observed in Table 5 that the values of D_i increase at higher temperatures, so that D_i values are 3.014×10^{-8}, 6.765×10^{-8}, 7.558×10^{-8}, and 9.191×10^{-8} m^2/s at 27, 45, 60, and 80 °C, respectively.
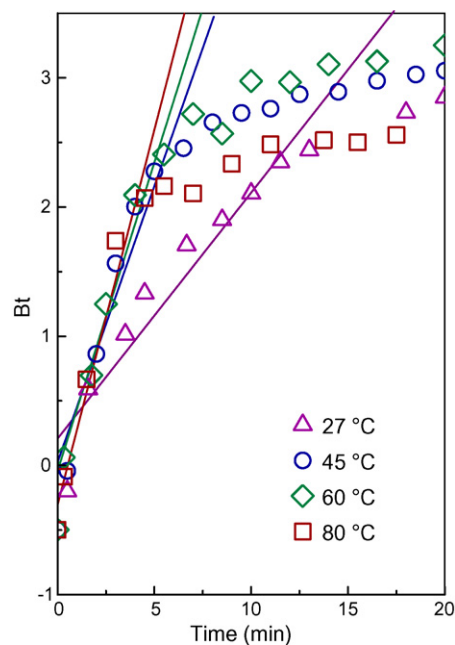

Fig. 11. Boyd plots for MB adsorption at different temperatures (pH 3.7–4.4; N-WH dose: 2 g/L; C_o: 97 mg/L).

4. Conclusions

1. The present study shows that nitric-acid treated water-hyacinth, an aquatic plant macrophyte, can be used as an adsorbent for the removal of methylene blue dye from aqueous solutions.
2. The amount of dye adsorbed was found to vary with initial methylene blue concentration, temperature, and contact time.
3. The amount of dye uptake (mg/g) was found to increase with the increase in contact time and initial MB concentration, but there is no linear relationship between the dye uptake and temperature.
4. The adsorption data was found to follow the pseudo second order kinetics at room temperature, but at higher temperatures both Lagergren's model and the pseudo second order model can be used to predict the adsorption kinetics.
5. The overall rate of dye uptake was found to be controlled by external mass transfer at the beginning of adsorption, then gradually changes to intraparticle diffusion controlled at a later stage.

References

[1] T. Robinson, G. McMullan, R. Marchant, P.R. Nigam, Remediation of dyes in textile effluent: a critical review on current treatment technologies with a proposed alternative, Bioresour. Technol. 77 (2001) 247–255.

[2] S.W. Won, S.B. Choi, Y. Yun, Interaction between protonated waste biomass of Corynebacterium glutamicum and anionic dye Reactive Red 4, Colloids Surf. A: Physicochem. Eng. Aspects 262 (2005) 175–180.

[3] Y.S. Ho, T.H. Chiang, Y.M. Hsueh, Removal of basic dye from aqueous solution using tree fern as a biosorbent, Proc. Biochem. 40 (2005) 119–124.

[4] G. McKay, J.F. Porter, G.R. Prasad, The removal of dye colours from aqueous solutions by adsorption on low-cost materials, Water Air Soil Pollut. 114 (1999) 423–438.

[5] K.V. Kumar, A. Kumaran, Removal of methylene blue by mango seed kernel powder, Biochem. Eng. J. 27 (2005) 83–93.

[6] K.S. Low, C.K. Lee, K.K. Tan, Biosorption of basic dyes by water hyacinth roots, Bioresour. Technol. 5 (1995) 79–83.

[7] P. Waranusantigul, P. Pokethitiyook, M. Kruatrachue, E.S. Upatham, Kinetics of basic dye (methylene blue) biosorption by giant duckweed (Spirodela polyrrhiza), Environ. Pollut. 125 (2003) 385–392.

[8] K.S. Low, C.K. Lee, The removal of cationic dyes using coconut husk as an adsorbent, Pertanika 13 (1990) 221–228.

[9] F. Banat, S. Al-Asheh, L. Al-Makhadmeh, Evaluation of the use of raw and activated date pits as potential adsorbents for dye containing waters, Process Biochem. 39 (2003) 193–202.

[10] D.S. De, J.K. Basu, Adsorption of methylene blue onto a low cost adsorbent developed from sawdust, Indian J. Environ. Prot. 19 (1998) 416–421.

[11] G. Annadurai, R. Juang, D. Lee, Use of cellulose based wastes for adsorption of dyes from aqueous solutions, J. Hazard. Mater. B92 (2002) 263–274.

[12] B. Gopal, Water Hyacinth, Elesevier, New York, NY, 1987.

[13] P.R. Epstein, Weeds bring disease to the East African waterways, Lancet 351 (1998) 577–586.

[14] A.M. El-Sayed, Effects of fermentation methods on the nutritive value of water of water hyacinth for Nile tilapia, *Oreochromis niloticus* (L.) fingerlings, Aquaculture 218 (2003) 471–478.

[15] P.S. Ganesh, E.V. Ramasamy, S. Gajalakshmi, S.A. Abbasi, Extraction of volatile fatty acids (VFAs) from water hyacinth using inexpensive contraptions, and the use of the VFAs as feed supplement in conventional biogas digesters with concomitant final disposal of water hyacinth as vermicompost, Biochem. Eng. J. 27 (2005) 17–23.

[16] A. Grandi, Use of Water Hyacinth in diets for rabbits, Coniglicoltura 18 (1981) 43–48.

[17] S. Lagergren, Zur theorie der sogenannten adsorption geloster stoffe. 591. Kungliga Svenska Vetenskapsakademiens, Handlingar 24 (4) (1898) 1–39.

[18] Y.S. Ho, Adsorption of heavy metals from waste streams by peat, Ph.D. Thesis, University of Birmingham, Birmingham, U.K., 1995.

[19] J. Bujdak, P. Komadel, Interaction of methylene blue with reduced charge montmorillonite, J. Phys. Chem. B 101 (1997) 9065–9068.

[20] A.P.P. Cione, M.G. Neumann, F. Gessner, Time-dependent spectrophotometric study of the interaction of basic dyes with clays: III. Mixed dye aggregates on SWy-1 and laponite, J. Colloid Interf. Sci. 198 (1998) 106–112.

[21] D. Mohan, K.P. Singh, Single and multicomponent adsorption of cadmium and zinc using activated carbon derived from bagasse-an agricultural waste, Water Res. 36 (2004) 2304–2318.

[22] W.J. Weber Jr., J.C. Morris, Kinetics of adsorption on carbon from solution, J. Sanitary Eng. Div. Proceed. Am. Soc. Civil Eng. 89 (1963) 31–59.

[23] Y.S. Ho, G. McKay, The Kinetics of sorption of basic dyes from aqueous solution by Sphagnum moss peat, Can. J. Chem. Eng. 76 (1998) 822–827.

[24] J.A. Medley, M.W. Andrews, The effect of a surface barrier on uptake rates of dye into wool fibers, Textile Resour. J. 29 (1959) 398–403.

[25] G.E. Boyd, A.W. Adamson, L.S. Myers Jr., The exchange adsorption of ions from aqueous solutions by organic zeolites, II: kinetics, J. Am. Chem. Soc. 69 (1947) 2836–2848.

[26] K. Banerjee, P.N. Cheremisinoff, S.L. Cheng, Adsorption kinetics of *o*-xylene by flyash, Water Res. 31 (1997) 249–261.